b_{to} and b_c are the thicknesses of the thermal mixing layer, equal to the distance along the y axis from t_{in} to t_{out} and from $t_{s\,in}$ to $t_{s\,out}$, respectively;

P_0 is the steam pressure in the nozzle forechamber;

ΔP is the pressure drop between the water ambient and points in the mixing layer.

LITERATURE CITED

1. J. Böhm, Gesund. Ing., No. 28 (1939).
2. P. A. Vecherskii, "Investigation of the thermal and hydrodynamic phenomena accompanying the outflow of steam into a liquid," in: Transactions of the Kiev Technological Institute of the Food Industry [in Russian], Vol.3 (1940).
3. F. T. Binford, L. E. Stanford, and C. C. Webster, Oak Ridge National Laboratory, ORNL-4374, UC-80-Reactor Technol. (1968).
4. P. J. Kerney, G. M. Faeth, and D. R. Olson, "Penetration characteristics of a submerged steam jet," AIChE J., 18, No. 3 (1972).
5. B. F. Glikman, "Experimental investigation of the condensation of a steam jet in liquid-filled space," Izv. Akad. Nauk SSSR, Otd. Tekh. Nauk, Energ. Avtom., No. 1 (1959).
6. B. F. Glikman, "Condensation of a steam jet in liquid-filled space," Izv. Akad. Nauk SSSR, Otd. Tekh. Nauk, No. 2 (1957).
7. Akio Kudo, Tatsuo Egusa, and Saburo Toda, "Basic study on vapor suppression. Heat transfer," in: Proceedings of the Fifth International Heat Transfer Conference, Tokyo, 1974, Vol. 3 (1974).
8. V. E. Nakoryakov and N. S. Safarova, "Simple equation for determining the position of the interface of phases in condensation of a submerged steam jet," Izv. Sib. Otd. Akad. Nauk SSSR, Ser. Tekh. Nauk, 8, No. 2 (1975).

INVESTIGATION OF SUBMERGED TURBULENT GAS JETS WITH DIFFERENT DENSITIES

V. A. Golubev and V. F. Klimkin

UDC 532.525.2

The results obtained in measuring the parameters in transverse sections and along the axis of submerged helium, air, and Freon jets are given along with the trends in the variation of the apparent additional mass of these jets.

Although the investigation of turbulent submerged jets has been treated in many papers [1-4], some problems concerning the trends of their propagation have not yet been resolved. We provide here the results of investigations of helium, air, and Freon jets and the generalization of certain characteristics of jets with different densities. Figure 1 shows the distribution of fields of the velocity head $q = \rho U^2/2$, the enthalpy i (or the temperature T), the concentration C (%), and the velocity U in transverse sections of helium, air, and Freon jets, measured in the main part of the jet at distances of 50, 70, 95, 120, and 145 mm from the nozzle cutoff. The jets of the above gases flow into an air atmosphere vertically upward from a profiled nozzle with the diameter d_j = 5 mm with fourfold contraction. The parameters of the operating conditions for the investigated jets are given in Table 1.

The velocity head in the jet is measured by means of a total-pressure tube, while the temperature is measured by means of a thermocouple. The concentration of admixtures in the helium jet is measured by means of a receiver with a tungsten filament, which is connected to a resistance bridge circuit.

The velocity U, the density ρ, and the enthalpy i in the jet are determined by measuring the velocity head $\rho U^2/2 = q$, the temperature T, and the concentration C. The Freon concentration by weight is calculated on the basis of measurements of the mixture temperature T_{mi} by means of the relationship [6]

Sergo Ordzhonikidze Moscow Aviation Institute.

Translated from Inzhenerno-Fizicheskii Zhurnal, Vol. 34, No.3, pp. 493-499, March, 1978. Original article submitted March 17, 1977.

0022-0841/78/3403-0333$07.50

TABLE 1. Parameters of the Operating Conditions for the Jets

Working fluid in jet	Legend	T_j, K	T_0, K	ρ_j, kg/m³	ρ_j/ρ_0	U_j, m/sec	$R_j \cdot 10^{-4}$	$G_j \cdot 10^3$, kg/sec	$q=\frac{\rho_j U_j^2}{2}$, N/m²
Helium	○	330	290	0,145	0,127	225	0,78	0,65	3750
Helium	□	330	«	0,145	0,122	600	2,1	1,71	26600
Air	△	337	«	1,03	0,86	85	2,15	1,71	3750
Air	▽	357	«	1,03	0,83	225	5,4	4,44	26600
Freon	◇	340	«	3,1	2,6	49	5,2	2,96	3750

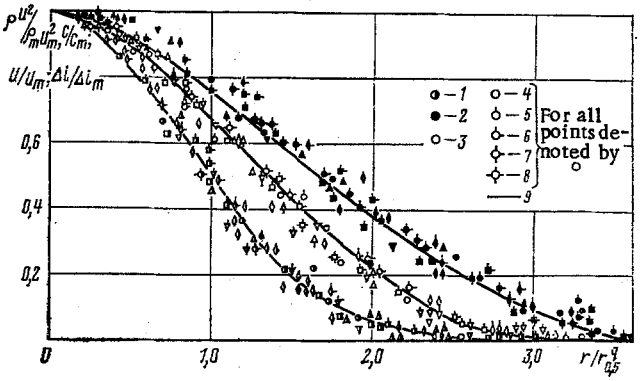

Fig. 1. Profiles of the dimensionless velocity head $\rho U^2/\rho_m U_m^2$ (1), the concentration C/C_m (2), the excess enthalpy $\Delta i/\Delta i_m$ (2) or the temperature T/T_m (2), and the velocity U/U_m (3) in transverse sections of the jet for different gases; 4) $x/r_j = 20$; 5) $x/r_j = 28$; 6) $x/r_j = 38$; 7) $x/r_j = 48$; 8) $x/r_j = 58$; 9) calculation.

$$C_F = \frac{c_{pa}T_{mi} - c_{pa}T_a}{T_{mi}(c_{pa} - c_{pF}) + (c_{pF}T_F - c_{pa}T_a)}, \quad (1)$$

where T_F and T_a are the temperatures of Freon at the nozzle cutoff and of the air ambient, respectively, and c_{pF} and c_{pa} are the specific heat values for Freon and air at the above temperatures, respectively.

The mixture density in helium and Freon jets is determined by means of the equation

$$\rho = \frac{\rho_i \rho_a}{C_i \rho_a + (1 - C_i)\rho_i}, \quad (2)$$

where C_i is the concentration by weight of helium or Freon, and ρ_i and ρ_a are the densities of helium or Freon and air at the temperature of the mixture, respectively.

The velocity in the jet is calculated by means of the expression

$$U = \sqrt{\frac{2q}{\rho}} \text{ (m/sec)}, \quad (3)$$

where q is the difference between the total pressures in the jet and the ambient (N/m²).

The enthalpy of the jet is determined by means of the expression

$$i = [C_i c_{pi} + (1 - C_i)c_{pa}]\, T_{mi}, \quad (4)$$

where c_{pi} and c_{pa} are the specific heat values for helium or Freon and air at the temperature of the mixture, respectively.

It is evident from the results given in Fig. 1 that the dimensionless profiles of the velocity head $\rho U^2/\rho_m U_m^2$, the velocity U/U_m, the enthalpy i/i_m or the temperature T/T_m, and the concentration C/C_m in helium, air, and Freon jets are affine with respect to length and similar with respect to the Reynolds number. The profiles of

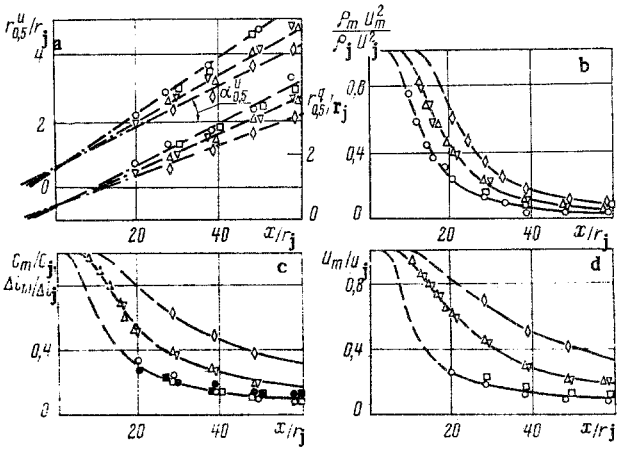

Fig. 2. Variation of the dynamic half-boundaries $r^q_{0.5}/r_j$ and $r^U_{0.5}/r_j$ (a) and of the axial parameters $\rho_m U_m^2/\rho_j U_j^2$ (b), C_m/C_j or $\Delta i_m/\Delta i_j$ (c), and U_m/U_j (d) along helium, air, and Freon jets for values of q equal to 3750 and 26,600.

dimensionless enthalpies (temperatures) for the investigated gases coincide with the concentration profiles; i.e., the trends in the transfer of heat and admixture concentration are identical. The transfer of heat and admixture concentration is more intensive than the momentum transfer; i.e., the thermal width of the jet is larger than the velocity width.

The dimensionless velocity in transverse sections of the jet, plotted on the basis of measurement results, is described by a theoretical profile determined by the expression

$$\frac{U}{U_m} = \left[1 - \left(0.44\,\frac{r}{r^U_{0.5}}\right)^{1.5}\right]^2, \tag{5}$$

while the results of temperature and concentration measurements are described by a theoretical profile calculated by means of

$$\frac{i}{i_m} = \frac{T}{T_m} = \frac{C}{C_m} = \left[1 - \left(0.44\,\frac{r}{r^C_{0.5}}\right)^{1.5}\right]^2. \tag{6}$$

In Eq. (5), the figure 0.44 represents the ratio of the transverse coordinate of the point $r^U_{0.5}$ where the jet velocity amounts to one-half of the maximum velocity to the coordinate of the limiting point r^U_{li} with zero velocity $r^U_{li}\left(r^U_{0.5}/r^U_{li} = 1.35/3.07 = 0.44\right)$; in Eq. (6), this figure corresponds to the ratio of the coordinate $r^C_{0.5}$ with half the excess enthalpy (temperature) or concentration to the limiting coordinate r^C_{li} with zero excess enthalpy or concentration $r^C_{li}\left(r^C_{0.5}/r^C_{li} = 1.64/3.77 = 0.44\right)$. The relationship between the coordinates $r^U_{0.5}$ and $r^C_{0.5}$ is determined by the turbulent Prandtl number (see Fig. 1):

$$\mathrm{Pr}_t = \frac{r^U_{0.5}}{r^C_{0.5}} = \frac{1.35}{1.64} = 0.82.$$

The longitudinal variation of the transverse coordinates where the velocity head amounts to one-half of the maximum head, $r^q_{0.5}$ and $r^U_{0.5}$, for helium, air, and Freon jets is shown in Fig. 2a. It is evident from the diagram that, with a reduction in the density of the working fluid in the jet, the apex angle α of the jet and its width r increase, while the distance to the pole l_0 diminshes. This distance is equal to $l_0 = 6.5\,r_j$ for a helium jet and $9r_j$ for Freon. The coordinate ratio $r^q_{0.5}/r^U_{0.5}$ for the investigated jets is equal to 0.74 ($r^q_{0.5}/r^U_{0.5} = 1/1.35 = 0.74$) (see Figs. 1 and 2a).

Figure 2b shows the axial variation of the measured values of the relative velocity head $\rho_m U_m^2/\rho_j U_j^2$ for helium, air, and Freon jets. The sharper decrease in the value of $\rho_m U_m^2/\rho_j U_j^2$ for helium jets ($\rho_j \approx 0.145$ kg/m^3) is connected with the longitudinal increase in the jet density. In Freon jets ($\rho_j = 3.1$ kg/m^3), the decrease of $\rho_m U_m^2/\rho_j U_j^2$ is much smaller than in an air jet ($\rho_j \simeq 1.0$ kg/m^3), which is connected with a drop in density along the jet. On the basis of the condition of momentum conservation, we obtain the equation:

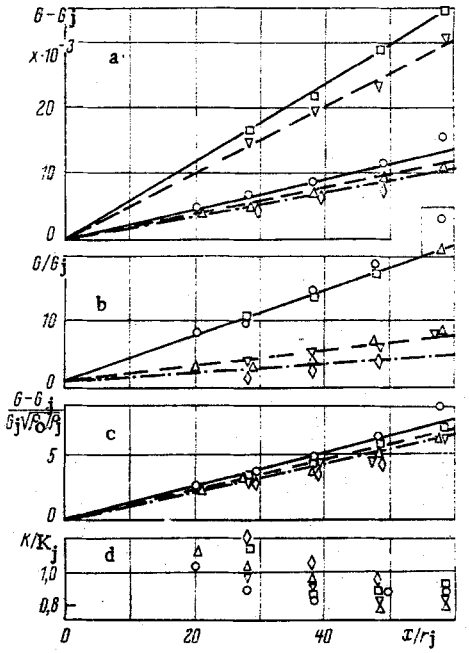

Fig. 3. Longitudinal variation of the apparent additional mass $G - G_j$, kg/sec (a), the relative discharge G/G_j (b), the grouping $(G - G_j)/G_j\sqrt{\rho_o/\rho_j}$ (c), and the momentum K/K_j (d) for helium, air, and Freon jets with q = 3750 and q = 26,600. The solid, dashed, and dash–dot curves pertain to helium, air, and Freon respectively (calculations based on (11).

$$\left(\frac{r^q_{0.5}}{r_j}\right)^2 \cdot \frac{\rho_m U_m^2}{\rho_j U_j^2} \int_0^{r^q_{1i}} 2\,\frac{\rho U^2}{\rho_m U_m^2} \cdot \frac{r}{r^q_{0.5}} \cdot \frac{dr}{r^q_{0.5}} = 1. \qquad (7)$$

As a result of graphic integration based on Fig. 1, we find that the integral is equal to 1.45. Knowing the value of the integral and using the plot of $r^q_{0.5}/r_j$ along the jets of helium, air, and Freon, we calculate by means of (7) the values of the relative velocity head $\rho_m U_m^2/\rho_j U_j^2$ along the jet axis and compare the theoretical and the experimental data.

The variation of the relative concentration C_m/C_j and the relative excess enthalpy $\Delta i_m/\Delta i_j$ is shown in Fig. 2c. The concentration in the Freon jet is calculated by means of (1) with respect to the results of temperature measurements, while the concentration in the helium jet is obtained by means of direct measurements and by using (1). It is evident from the diagram that the results of concentration measurements in helium jets coincide with theoretical data. The variations of the relative axial concentration C_m/C_j and the relative excess enthalpy $\Delta i_m/\Delta i_j$ are identical in these jets. The longitudinal drop in the relative velocity U_m/U_j at the axis is shown in Fig. 2d. The velocity is calculated by means of Eq. (3).

The experimental measurements indicate that, for a Freon jet ($\rho_j/\rho_o = 3.1$), the relative velocity at the axis is equal to $U_m/U_j = 0.9$ for $x/r_j = 20$, while, for instance, in a plasma jet ($\rho_j/\rho_o = 0.004$), $U_m/U_j = 0.1$ for the same value of x/r_j [5].

Figure 3a shows the experimental data on the variation of the apparent additional mass of the investigated jets along the axis. It follows from these data that the mass driven by the jet is the larger, the greater the momentum $K_j = \rho_j U_j^2$ possessed by the jet at the nozzle outlet (for equal orifice diameters).

For equal initial momentums, the rate at which the apparent additional mass increases is higher in jets with low density than in jets with high density. The latter is explained by the fact that the outflow velocity increases as the jet density diminishes. It should be noted that air jets with q = 26,600 and helium jets with q = 3750 have equal outflow velocities, while air jets with q = 3750 and helium jets with q = 26,600 have equal initial gas discharges through the nozzle.

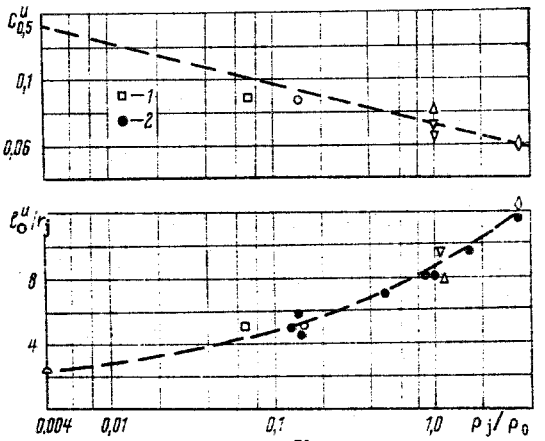

Fig. 4. Coefficients $C^U_{0.5}$ and initial section length l^U_o/r_j as functions of the jet density. 1) Based on (10); 2) after V. I. Kukes.

The relative values of the apparent additional mass G/G_j for the investigated jets (see Fig. 3b) are independent of the initial momentum, and they coincide for q = 26,600 and q = 3750; i.e., the relative apparent additional mass is determined only by the density of the working fluid in the jet (Fig. 3b). The increment of the apparent additional mass of the jet over the length Δx is determined by means of the expression [7]

$$\Delta G = G - G_j = 2\pi r^U_{1i}\, \rho_o v \Delta x, \tag{8}$$

where v is the transverse inflow velocity at the jet boundary. Expression (8) can be represented in dimensionless form:

$$\frac{\Delta G}{G_j} = 2\,\frac{r^U_{1i}}{r_j}\,\frac{\rho_o}{\rho_j}\,\frac{U_m}{U_j}\,\frac{v}{U_m}\,\frac{\Delta x}{r_j}. \tag{9}$$

Assuming that the relative inflow velocity for the investigated jets is constant along the length and equal to $v/U_m = 0.02$, we use the diagrams of $r^U_{0.5}/r_j$ and U_m/U_j (see Fig. 2a and d) to calculate by means of Eq. (9) the values of the apparent additional mass for helium, air, and Freon jets, which are in satisfactory agreement with experimental data.

In view of the large volume of calculations, it is more convenient to use the expression derived on the basis of dimensional theory, which is given in [9]:

$$\frac{G}{G_j} = 0.32\,\frac{x}{d_j}\sqrt{\rho_o/\rho_j}. \tag{10}$$

This expression ensures good agreement with experimental data at large distances from the nozzle, but loses its physical meaning near the nozzle. Our experimental values are somewhat lower than those obtained in [9], which is possibly connected with errors in measuring the velocities, especially in peripheral jet zones. Therefore, for better agreement with experimental data, the apparent additional mass is determined by means of the expression

$$\frac{G - G_j}{G_j} = 0.275\,\frac{x}{d_j}\sqrt{\rho_o/\rho_j}. \tag{11}$$

Figure 3c shows the variation of the apparent additional mass, reduced to the gas discharge through the nozzle, with a correction for the difference between the densities of the jet gas and the ambient. However, in contrast to what has been found in [8], the grouping $G - G_j/G_j\sqrt{\rho_o/\rho_j}$ separates into individual branches for the investigated jets. The values of the relative momentum K/K_j along the jet are given in Fig. 3d. The slight differences between the calculated values and unity are connected with errors in measuring the velocity heads, temperatures, and concentrations in transverse jet sections.

Figure 4 shows the coefficient $C^U_{0.5}$ of the submerged jet, where the velocity is equal to one-half of the axial velocity, and the initial section length obtained from measurements of the velocity head or the velocity l^U_o/r_j as functions of the jet density. Considering that the velocity profile is described by (5), the jet boundary with respect to velocity is determined by the relationship:

$$c_{1i}^{U} = \frac{c_{0.5}^{U}}{0.44}.$$

The initial section length for a plasma jet ($\rho_j/\rho_0 = 0.004$) is negligible; it is equal to $l_0^U/r_j = 3.1$ [5]. The initial section length obtained by measuring temperatures or concentrations is smaller than l_0^U by 1.5-2.0 nozzle radii.

The above results make it possible to calculate and plot the behavior of the basic parameters in the transverse sections of jets at various distances from the nozzle in a wide range of densities.

NOTATION

r_j	is the nozzle radius;
x	is the distance along the jet axis;
r	is the jet radius;
U_j	is the jet velocity at the nozzle outlet (m/sec);
ρ_j and ρ_0	are the densities of the jet and the ambient, respectively;
$q = \rho_j U_j^2/2$	is the velocity head of the jet at the nozzle outlet;
$K_j = \rho_j U_j^2$	is the jet momentum at the nozzle outlet per unit area;
C	is the concentration by weight of the helium or Freon admixture in the jet;
G_j	is the jet mass at the nozzle outlet;
v	is the transverse inflow velocity at the jet boundary.

LITERATURE CITED

1. G. N. Abramovich, Turbulent Jet Theory [in Russian], Fizmatgiz (1960).
2. G. N. Abramovich (editor), Turbulent Mixing of Gas Jets [in Russian], Nauka (1974).
3. L. A. Vulis and V. P. Kashkarov, Theory of Viscous Liquids Jets [in Russian], Nauka (1965).
4. G. N. Abramovich (editor), Investigation of Turbulent Air, Plasma, and Propulsion Gas Jets [in Russian], Mashinostroenie (1967).
5. G. N. Abramovich, V. I. Bakulev, V. A. Golubev, and G. G. Smolin, "Investigation of submerged turbulent jets in a wide temperature range," Int. J. Heat Mass Transfer, 9, 1047 (1966).
6. K. A. Malinovskii, Mekh. Zhidk. Gaza, No. 1 (1967).
7. O. V. Yakovlevskii, Izv. Akad. Nauk SSSR, Otd. Tekh. Nauk, Mekh. Mashinostr., No. 3 (1961).
8. I. B. Palatnik and D. Zh. Temirbaev, in: Problems of Heat Engineering and Applied Thermophysics [in Russian], Vol. 4, Nauka, Alma-Ata (1967).
9. F. P. Ricou and D. B. Spalding, J. Fluid Mech., II, Part 1 (1961).
10. V. Ya. Bezmenov and V. S. Borisov, "Turbulent air jet heated to 4000°K," Izv. Akad. Nauk SSSR, Otd. Tekh. Nauk, Ser. Energ. Avtom., No. 4 (1961).